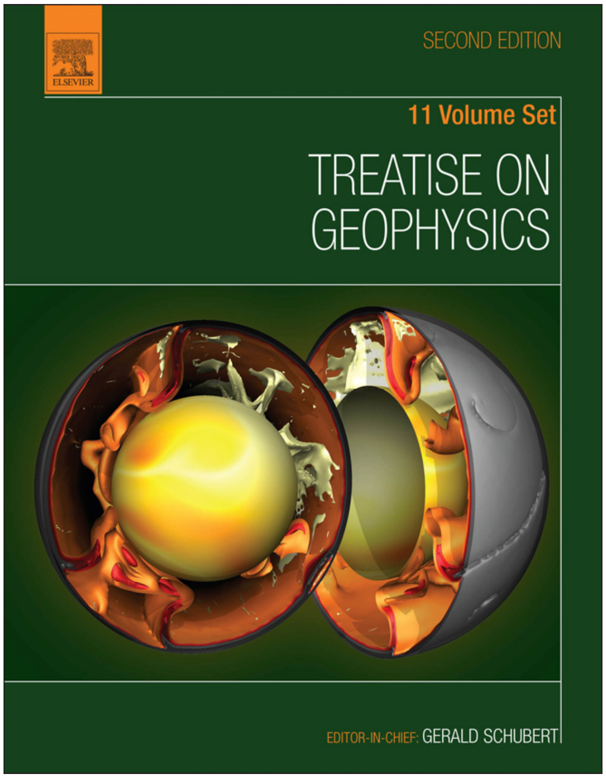

Buffett B.A Core–Mantle Interactions. In: Gerald Schubert (editor-in-chief) Treatise on Geophysics, 2^{nd} edition, Vol 8. Oxford: Elsevier; 2015. p. 213-224.

8.08 Core–Mantle Interactions

BA Buffett, University of California, Berkeley, CA, USA

8.08.1 Introduction

Two giant heat engines operate inside the Earth. One powers plate tectonics and accounts for most of the geologic phenomena we observe at the surface. The other operates in the core, where it continually sustains the Earth's magnetic field against persistent ohmic losses. These two heat engines are coupled, primarily through interactions at the boundary between the core and mantle. Transfer of heat, mass, momentum, and electric current across the boundary profoundly affects the dynamics and evolution of both regions on timescales ranging from days to hundreds of millions of years. On short timescales, we observe diurnal wobbles in the Earth's rotation, which are strongly affected by relative motion between the core and the mantle (e.g., Mathews and Shapiro, 1992). This and other types of mechanical interaction influence the flow in the core (e.g., Calkins et al., 2012) and contribute to variations in the length of day (see **Chapter 8.04**). On longer timescales, we expect variations in both the magnitude and spatial distribution of heat flow across the boundary. The resulting thermal interactions influence the vigor and pattern of convection in the core and may alter the frequency of reversals (Glatzmaier et al., 1999; Olson et al., 2010). Electromagnetic interactions are also possible, particularly if the lowermost mantle has a large electrical conductivity. Electric currents near the base of the mantle can generate both large- and small-scale magnetic fields, while the associated Lorentz force contributes to the mechanical interaction. More recent suggestions of chemical reactions between the core and mantle (Brandon and Walker, 2005; Ozawa et al., 2009) raise the intriguing but contentious suggestion that mass has been transferred between the two regions over geologic time. In this chapter, we focus on the consequences of core–mantle interactions for processes in the core. We address a number recent advances in our understanding of thermal, mechanical, electromagnetic, and chemical interactions, as they relate to the dynamics and evolution of the core. We also deal with the role of core–mantle interactions as a means of detecting deep-earth processes at the surface.

8.08.2 Thermal Interactions

Heat flow across the core–mantle boundary (CMB) is a fundamental parameter for the evolution of the core. It controls the rate of cooling and solidification of the core and determines the vigor of convection in the fluid outer core (Nimmo, **Chapter 8.02**). Convection is driven by a combination of thermal and chemical buoyancies as the fluid core cools and solidifies. Chemical buoyancy arises through the exclusion of the light elements from the growing inner core (Braginsky, 1963), whereas thermal buoyancy is generated by latent heat release on solidification (Verhoogen, 1961) and by forming cold, dense fluid in the thermal boundary layer at the top of the core. Each of these buoyancy sources is paced by the CMB heat flow.

The mantle plays an important role in regulating the magnitude of CMB heat flow. The large and relatively sluggish mantle limits heat loss from the core. Estimates of the CMB heat flow are often obtained from inferences of the temperature jump across the thermal boundary layer on the mantle side of the interface (e.g., Lay et al., 2008). Typical values of the heat flow are 6–16 TW, although our present state of knowledge is not sufficient to rule out higher or lower values. Such a broad range of values permit two distinct styles of convection in the core (see **Figure 1**). One style occurs when the CMB heat flow exceeds the conduction of heat along the adiabatic gradient at the top of the core (denoted by Q_{ad}). Convection carries heat in excess of that transported by conduction, requiring a thermal boundary layer on the core side of the boundary. This provides a source of cold, dense fluid to drive convection from the top down into the core. The other regime occurs when the CMB heat flow is less than Q_{ad}. In this case, the mantle is unable to remove the heat carried by conduction down the adiabat. Excess heat accumulates at the top of the core (Gubbins et al., 1982) or is mixed into the interior by flows driven by chemical buoyancy (Loper, 1978). Either of these possibilities eliminates thermal buoyancy production at the top of the core, restricting the buoyancy production to the inner-core boundary region.

Estimates for Q_{ad} have undergone substantial revision in the past few years. Values of Q_{ad} in the range of 5–6 TW are typically obtained when the thermal conductivity is 40–50 W m^{-1} K^{-1}. Higher thermal conductivities from recent theoretical studies (de Koker et al., 2012; Pozzo et al., 2012) yield values of $Q_{ad} = 12$–14 TW. Such a high value could exceed the CMB heat flow. It is also possible that the magnitude of Q_{ad}, relative to the total CMB heat flow, has changed with time. For example, a higher CMB heat flow is likely in the early Earth. Indeed, a higher heat flow

 http://dx.doi.org/10.1016/B978-0-444-53802-4.00148-2
Treatise on Geophysics, *2nd edition*, *(*2015), vol. 8, pp. 213-224

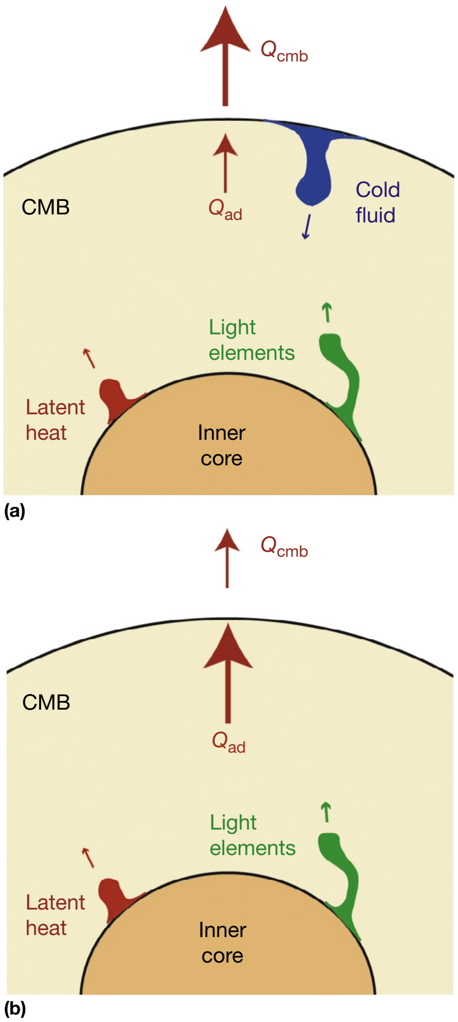

Figure 1 Two distinct styles of convection operate in the core, depending on the relative magnitude of the CMB heat flow, Q_{cmb}, and the heat flow conducted down the adiabat at the CMB, Q_{ad}. a) A thermal boundary layer forms at the top of the core when $Q_{cmb} > Q_{ad}$. Cold and dense fluid at the CMB drives convection from the top. Latent heat and compositional buoyancy from the inner-core boundary drive convection from the bottom. b) The thermal source of buoyancy at the top of the core disappears when $Q_{cmb} < Q_{ad}$. The excess heat that is carried to the CMB by conduction either accumulates at the top or is mixed back into the interior by compositional buoyancy.

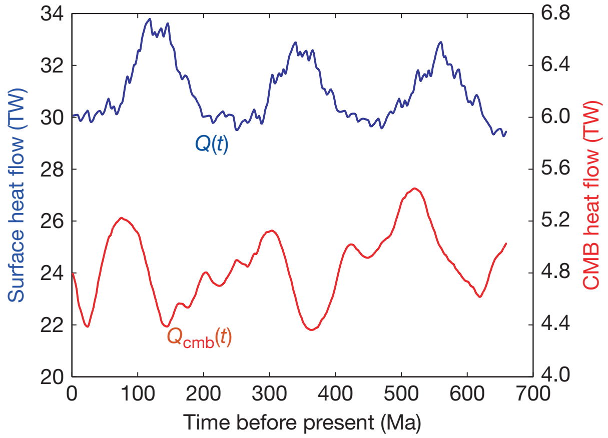

Figure 2 Heat flow at the surface $Q(t)$ and the CMB $Q_{cmb}(t)$ from a numerical convection model with imposed plate motions (Bunge et al., 2003). Plate motion histories over the past 120 Ma are cyclically repeated at earlier times to assess the response with different initial conditions. High heat flow at the surface coincides with times of faster than average plate spreading rates. Increases in heat flow at the CMB occur 50 to 60 Ma later.

may be essential to power the dynamo prior to the formation of the inner core. A switch to bottom-driven convection in the core becomes possible as the Earth cools and the inner core grows.

We might even expect the style of convection to switch intermittently between regimes if the current CMB heat flow is sufficiently close to Q_{ad}. Fluctuations in mantle convection can transiently shift the CMB heat flow above or below Q_{ad}, altering the convective regime.

Evidence for fluctuations in mantle convection can be found in geologic estimates of plate motions. Estimates from the past 120 million years suggest that spreading rates have generally decreased over this time, perhaps by more than 20% (Lithgow-Bertelloni and Richards, 1998; Xu et al., 2006). While the magnitude of this change is debated (Heller et al., 2006; Rowley, 2002), it is clear that modest fluctuations in plate motion can cause thermal interactions with the core. The size and timing of these interactions can be explored by incorporating estimates of plate motions into numerical models of mantle convection (Bunge et al., 2003; McNamara and Zhong, 2005; Zhang and Zhong, 2011). The overall amplitude of CMB heat flow in numerical models can vary widely with the choice of viscosity profile and CMB temperature. However, changes in the rate of plate motion invariably produce changes in the CMB heat flow. Figure 2 shows the predicted change in heat flow at the surface and at the CMB when plate motions are varied in time according to the calculations of Bunge et al. (2003). (The plate motions over the past 120 Ma are cyclically repeated to extend the record back in time and explore solutions with different initial conditions.) High heat flow at the surface coincides with times of rapid plate spreading. Changes at the CMB are felt about 50–60 Ma later, reflecting the sinking time of subducted lithosphere. A somewhat shorter delay of 30 Ma is reported in the study of Zhang and Zhong (2011). Such a simple correspondence between surface plate speeds and CMB heat flow is probably a crude approximation of the actual dynamics. If the pace of mantle convection is connected with the rates of magnetic reversals, then some incoherence between plate motion and CMB heat flow is required to explain why prolonged periods of dipole stability (i.e., superchrons) are associated with both fast and slow plate speeds (Olson et al., 2013). For the results shown in Figure 2, the variation in CMB heat flow is roughly 1 TW, or about 20% about the time-averaged value.

Changes in the CMB heat flow alter the supply of thermal and chemical buoyancies in the outer core. A stratified layer at the top of the core can develop when the heat flow drops below Q_{ad} because the mantle can no longer keep pace with the heat supplied from below by conduction along the adiabat in the core. Excess heat accumulates at the top of the core unless convection in the core can entrain warm fluid back into the interior. In the absence of entrainment, we expect a warm, stratified layer to grow in response to changes in densities inside and below the stratified layer (Lister and Buffett, 1998). Heat accumulates in the stratified layer, causing the warm fluid to encroach down into the underlying convective region. However, light elements from the inner-core boundary accumulate in the convective region, so the stratified layer gradually becomes heavier in terms of composition. This interplay between the thermal and chemical buoyancies ultimately limits the growth of the stratified layer.

Figure 3 shows two predictions for the thickness of a stratified layer using the model of Lister and Buffett (1998). For the sake of illustration, we adopt the CMB heat flow $Q_{\mathrm{cmb}}(t)$ from Figure 2 and consider two conventional values for Q_{ad}. Qualitatively similar results are obtained using the recent theoretical values for Q_{ad} and a higher CMB heat flow, $Q_{\mathrm{cmb}} \sim 13–14$ TW, from the study of Zhang and Zhong (2011). A lower value, $Q_{\mathrm{ad}} = 5$ TW, causes an intermittent stratified layer to develop whenever $Q_{\mathrm{cmb}}(t)$ drops below Q_{ad}. A permanent stratified layer develops when $Q_{\mathrm{ad}} = 6$ TW, although the thickness of the layer fluctuates in time. In both examples, there is a lag between the time when Q_{cmb} is low and the time when the stratified layer reaches its maximum thickness. This time lag is set primarily by the thermal diffusion time for the stratified layer. We find a relatively thick stratified layer at 100–110 Ma, following a low CMB heat flow at 130 Ma. The low CMB heat flow (in this model) is a consequence of slow plate motions at the surface, 50–60 Ma earlier. The thickest layers are predicted to coincide with the time of maximum surface heat flow, although this result depends on the timescale for variations in the surface heat flow. The existence of a stratified layer in the core might be inferred from observations of variations in the magnetic field, because a stable layer would filter magnetic fluctuations from the underlying convective region (Sreenivasan and Gubbins, 2008). Distinctive features in the field may also develop in the stratified layer through interactions with the convective flow in the underlying region (Zhang and Schubert, 2000). Even more dramatic consequences are possible if the change in CMB heat flow causes the geodynamo to fail. For example, Nimmo and Stevenson (2000) suggested that a transition from plate tectonics to stagnant lid convection on Mars was sufficient to suppress convection throughout the Martian core, causing a termination of the magnetic field.

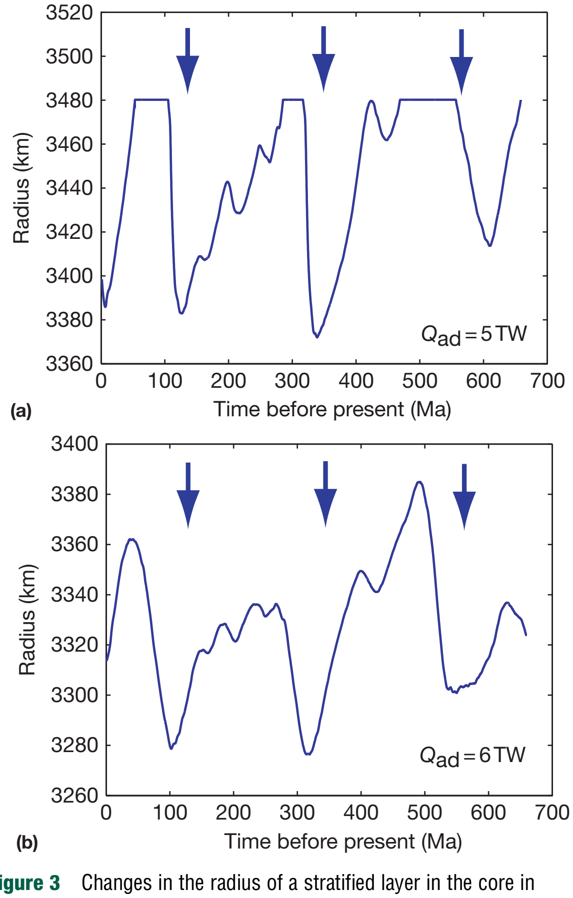

Figure 3 Changes in the radius of a stratified layer in the core in response to variations in CMB heat flow. a) The stratified layer vanishes when the CMB heat flow exceeds the adiabatic heat flow Q_{ad}. Under these conditions the radius of the stratified layer equals the radius of the core (e.g. 3480 km). The stratified layer reappears whenever the CMB heat flow drops below Q_{ad}. b) A persistent stratified layer is present when $Q_{\mathrm{ad}} = 6$ TW, although the thickness of the layer varies with time. The arrows indicate the times when the heat flow at the surface is maximum.

Lateral variations in heat flow at the CMB also affect the dynamics of the core. Cold slabs at the base of the mantle are expected to increase the local heat flow by increasing the magnitude of the local temperature gradient at the boundary. This effect seems unavoidable because the low viscosity of the core liquid maintains a nearly constant temperature over the boundary (Bloxham and Jackson, 1990). Small adiabatic variations in temperature over kilometer-scale topography produce temperature variations of roughly 1 K, but these variations are small compared with temperature anomalies of several hundred kelvin or more in the mantle. Consequently, variations in heat flow over the CMB can be inferred from the thermal structure on the mantle side of the boundary. Numerical simulations (Sarson et al., 1997; Zhang and Gubbins, 1993, 1996) and experiments (Sumita and Olson, 1999, 2002) show that lateral variations in heat flow drive fluid motion in the core. In fact, several studies have sought to interpret core flows obtained from secular variation of the magnetic fields in terms of regional variations in heat flow (Bloxham and Gubbins, 1987; Kohler and Stevenson, 1990). Numerical simulations of convection with lateral variations in heat flow reveal a tendency to lock the pattern of convection to the pattern of heat flow at the boundary, although this behavior typically occurs for a narrow range of parameter values. More commonly, the flow is highly time-dependent. The source of the time dependence appears to be a consequence of switching the flow between the horizontal scale of the imposed boundary conditions and the natural scale of convection (Sumita and Olson, 2002; Zhang and Gubbins, 1996).

Similar conclusions are drawn from numerical geodynamo models (Bloxham, 2002; Olson and Christensen, 2002; Sarson et al., 1997). Nonhomogeneous boundary conditions in geodynamo models yield persistent structure in the time-averaged flow (Bloxham, 2002; Davies et al., 2008; Olson and Christensen, 2002), although there can be substantial variation about the average (Bloxham, 2002; Christensen and Olson, 2003). The spatial pattern of the core flow is reflected in the structure of the magnetic field. Models that use seismic heterogeneity at the base of the mantle to infer the local heat flow have been successful in producing a magnetic field with persistent nondipole structure (see **Figure 4**), similar to that deduced from paleomagnetic observations over the past few million years (Gubbins and Kelly, 1993; Johnson and Constable, 1997, 1998). However, the persistent nondipole structure is not prominent in individual snapshots of the solution; it emerges only after averaging the time-dependent part of the field. So far, it has not been possible to use thermal interactions to explain stationary features in the historical field over the past 300 years (Bloxham, 2002).

Spatial variations in heat flow may also have an important influence on magnetic reversals. The study of Glatzmaier et al. (1999) showed that different patterns of heat flow at the CMB can alter the frequency of magnetic reversals. When the pattern of CMB heat flow is compatible with the natural pattern of convection in the outer core, there is a tendency to produce a stronger dipole field with less time dependence and fewer magnetic reversals. The opposite behavior is observed when the pattern of heat flow and the natural scale of convection are distinct; in this case, much larger variations are observed in the field and reversals appear more frequently. Somewhat surprisingly, the most realistic behavior, in terms of time variations in the virtual geomagnetic pole (VGP), was obtained with uniform boundary conditions. Such a model cannot explain the persistent nondipole structure of the field, so there appear to be other contributing factors. For example, Olson et al. (2010) showed that reversal rates are more sensitive to total heat flow than the spatial variations. High reversal rates correspond to high CMB heat flow, whereas the times of low CMB heat flow could plausibly coincide with extended periods of stable polarity (Driscoll and Olson, 2011).

Numerical models also suggest that dynamo action fails when lateral variations in heat flow become comparable to the average convective heat flow (Olson and Christensen, 2002). Because a large part of the heat flow at the CMB is carried by conduction along the adiabat, the convective part of the average heat flow could be quite small (or even negative). Lateral variations in heat flow could easily exceed the average convective heat flow, which appears to doom the magnetic field in thermally driven dynamo models. It is not presently known if the dynamo models would still fail if convection was driven primarily by compositional buoyancy. Reconciling the behavior of the field with plausible thermal interactions remains an outstanding challenge.

Another consequence of thermal interactions involves the behavior of the field during a reversal. Compilations of VGPs from transition fields suggest that the VGPs are clustered into one of two preferred longitudes during a reversal (Clement, 1991; Laj et al., 1991). In fact, it is possible for different sites to record different paths for the same reversal because the VGP location is based on the assumption of a dipole field. Nondipole (multipole) components of the field also contribute to the direction of the field at a given site, shifting the VGP location from the position of the actual dipole axis. Different reversal paths emerge from different sites when the multipole components become prominent relative to the dipole. Kutzner and Christensen (2004) investigated the question of preferred reversal paths using a geodynamo model with lateral variations in CMB heat flow. Part of the time-averaged magnetic field in this study included an equatorial dipole, which defines a preferred orientation in longitude. Modeled VGP paths from a large number of sites on the surface sense this orientation, causing a preferred path during reversals. However, the scatter in VGP directions due to multipole components means that the preferred direction emerges only when a large number of sites are averaged. The question of whether preferred reversal paths can be inferred from a small number of sites at the surface remains a contentious issue, both for the models and for the paleomagnetic observations. Additional questions arise because the models are still very far from earthlike conditions. On the other hand, the signatures of thermal core–mantle interactions should be embedded in the flow and field at the top of the core. Identifying these signatures in both observations and models should be an important part of future progress.

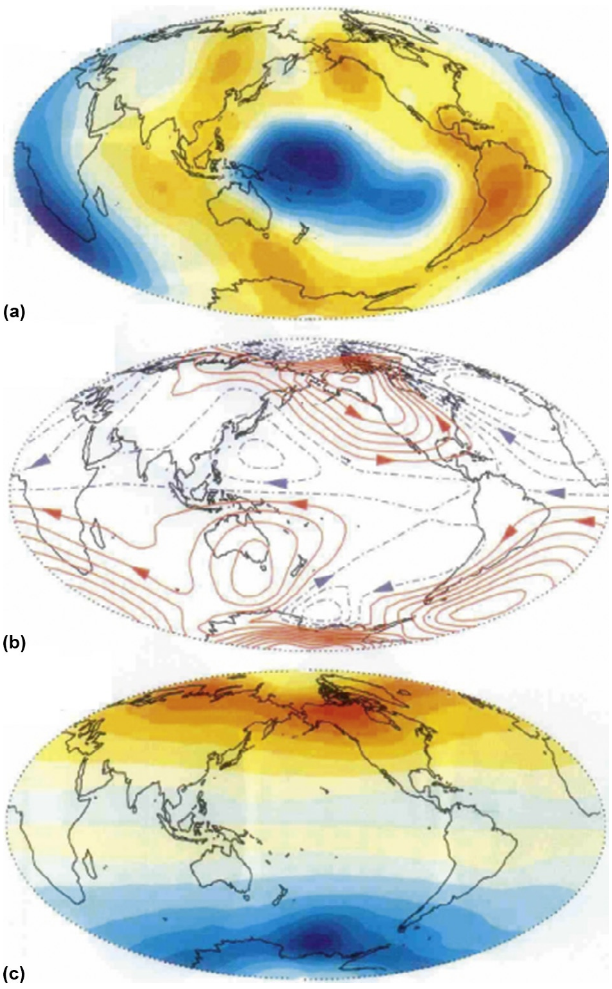

Figure 4 Lateral variations in Q_{cmb} induce flow near the top of the core and alter the time-averaged magnetic field from calculations of Olson and Christensen (2002). a) Lateral variations in boundary heat flow are based on seismic models of velocity heterogeneity near the CMB. b) Toroidal streamlines of steady flow below the CMB are due to imposed heat flow conditions. c) Time-averaged radial magnetic field at CMB reveals non-zonal structure.

8.08.3 Electromagnetic Interactions

Electric currents are induced in the lower part of the mantle as a consequence of dynamo action in the liquid core. Several types of interactions between the core and mantle are possible. One involves the force on current-carrying material, which can transfer momentum between the core and the mantle. This mechanism is commonly proposed to explain variations in the length of day over periods of several decades (e.g., Bullard et al., 1950). A second type of interaction causes a distortion the magnetic field as it diffuses through the mantle toward the surface. The importance of both effects depends on the electrical conductivity of the lower mantle.

Laboratory-based estimates for mantle silicates and oxides, extrapolated to lower mantle conditions, typically yield conductivities of 10 S m^{-1} or less (Xu et al., 2000). Such low values are expected to yield relatively weak currents in the lower mantle and small electromagnetic core–mantle interactions. However, more substantial electromagnetic interactions are possible if the lowermost mantle is not composed entirely of silicates and oxides. Chemical reactions between the core and mantle have been proposed as a mechanism to incorporate iron alloys into the base of the mantle (Knittle and Jeanloz, 1989). The iron alloy may be a reaction product (Jeanloz, 1990) or a result of incorporating core material directly into the mantle (Buffett et al., 2000; Kanda and Stevenson, 2006; Otsuka and Karato, 2012; Petford et al., 2005; Poirier and LeMouel, 1992). A new high-pressure phase of $MgSiO_3$ (Murakami et al., 2004; Oganov and Ono, 2004) may open other possibilities for high electrical conductivities in the lower mantle (Ohta et al., 2010; Ono et al., 2006). Regions of low conductivity may also arise from changes in the partition of iron between the dominant mineral components due to a transition in the spin state of iron in ferropericlase (Badro et al., 2003).

One of the earliest suggestions of electromagnetic core–mantle interaction was motivated by the observation of small fluctuations in the length of day over periods of several decades (Bullard et al., 1950; Rochester, 1962; Roden, 1963). Motion of the core relative to the mantle sweeps lines of magnetic field through the lower mantle, inducing a horizontal electric current. The resulting forces on the core and mantle act to oppose any relative motion. The axial component of the associated torque transfers angular momentum between the core and mantle. Stix and Roberts (1984) were the first to use detailed estimates of flow at the top of the core to determine the electromagnetic torque on the mantle. They predicted variations in the torque that were sufficient to explain the fluctuations in the length of day. However, these variations were superimposed on a steady torque, which had the undesirable effect of causing a steady change in the angular velocity of the core and the mantle. To avoid this effect, they proposed an additional (balancing) torque, which arises when radial electric currents leak across the CMB. The existence of such a current is reasonable, although it cannot be constrained by surface observations. As a result, electromagnetic interactions provide a viable but unproven mechanism for explaining decadal variations in the length of day.

Holme (1998) revisited the question of electromagnetic core–mantle interactions by showing that core flows inferred from measurements of secular variation could not constrain the torque on the mantle (also see Wicht and Jault, 1999). This means that any torque computed from a flow model is largely a product of the assumptions used to resolve the nonuniqueness of the flow rather than the measurements of secular variation. The strategy proposed by Holme (1998) was to determine the flow at the top of the core by fitting the observed secular variation subject to the condition that rearrangement of magnetic flux explains the length-of-day variations. (This calculation did not require any radial current across the CMB.) Plausible core flows were found to explain the variations in the length of day, provided the conductance of the lower mantle was roughly 10^8 S. The necessary conductance could be obtained with a 100 km layer at the base of the mantle and an average conductivity of 10^3 S m^{-1}, although other combinations of thickness and conductivity are possible.

A similar value for the conductance of the lower mantle was obtained from the study of the Earth's nutation (Buffett, 1992). Periodic variations in the direction of the Earth's rotation (nutations) are caused by the lunar and solar tides. The Earth's response to tidal torques includes a differential rotation of the core relative to the mantle, which alters the measured nutation. Electromagnetic interactions cause an additional perturbation by introducing a restoring force that opposes the differential rotation. The associated dissipation due to ohmic loss is detected as a phase lag in the response relative to that predicted for an elastic Earth model (e.g., Mathews and Shapiro, 1992). Comparison of theoretical predictions (Mathews et al., 1991; Wahr, 1981) and observations (Herring et al., 1991) reveals a large discrepancy in the annual nutation, which is particularly sensitive to relative motion between the core and the mantle. Including electromagnetic interactions could eliminate this discrepancy, as long as the conductance of the lower mantle is 10^8 S, comparable to the value required to explain length-of-day variations. However, there is one important distinction. Nutations involve nearly diurnal motion of the core relative to the mantle. (An annual nutation is defined by the period of the beat frequency between the nearly diurnal motion and exactly one cycle per day.) The associated skin depth for magnetic diffusion over diurnal periods limits electric currents to the immediate vicinity of the boundary, so the discrepancies in the nutations are most easily explained by high (10^5–10^6 S m^{-1}) conductivities in a relatively thin (10^2–10^3 m) layer. A variety of mechanisms have been examined to explain (or refute) such a conducting layer at the base of the mantle (Buffett et al., 2000; Kanda and Stevenson, 2006; Knittle and Jeanloz, 1991; Otsuka and Karato, 2012; Petford et al., 2005; Poirier and LeMouel, 1992). While improvements in nutation theory (Koot et al., 2008; Mathews et al., 2002) and observations (Herring et al., 2002) continue to support the existence of a conducting layer, other sources of dissipation have also been proposed. The most likely alternative is viscous dissipation in the liquid core (Buffett, 1992; Deleplace and Cardin, 2006; Koot et al., 2010; Mathews and Guo, 2005), although this explanation requires a viscosity that is roughly four orders of magnitude larger than recent estimates (de Wijs et al., 1998; Zhang and Guo, 2000).

Another type of electromagnetic interaction arises when the electrical conductivity in the lower mantle varies laterally. Steady flow in the core sweeps the radial (poloidal) component of the magnetic field through the mantle, inducing local electric currents. In a uniform conductor, these currents produce a tangential (toroidal) component of the magnetic field. However, a heterogeneous conductor directs current through the conducting regions. The added complexity in the path of electric current induces a poloidal field, which can strengthen the initial poloidal field. Busse and Wicht (1992) showed that self-sustaining dynamo action is possible in this case, even when the flow in the core is spatially uniform. In effect, the complexity of the conductivity structure replaces the need for complicated fluid motion in a uniform conductor. While the conditions required for self-sustaining dynamo action are unlikely to be realized in the Earth's core, it is possible to induce a small-scale radial field with an amplitude as large as 0.1 mT (Buffett, 1996a). This mechanism can also contribute to the large-scale field at the surface by distorting the unseen toroidal field to produce an observable poloidal component (Koyama et al., 2001). More recent geodynamo simulations with an electrically heterogeneous mantle suggest that the nondipole part of the magnetic field at the Earth's surface can be strongly affected by the distribution of conductivity in the mantle (Chan et al., 2008).

Electromagnetic interactions also accompany time variations in the amplitude of the magnetic field. The largest change in amplitude probably occurs during magnetic reversals. While the general structure of the field during a reversal is not well known, we do know that the axial part of the dipole field vanishes and reappears with the opposite polarity in as little as several thousand years (Clement, 2004; Valet et al., 2012). Rapid time variations in the axial dipole create large-scale electric fields in the lower mantle. When the distribution of electrical conductivity of the mantle is heterogeneous, the resulting currents generate a poloidal field (see **Figure 5**). The structure of the induced field depends on the spatial distribution of electrical conductivity. A large-scale pattern of electrical conductivity with a local conductance of 10^8 S should produce an observable field during a magnetic reversal. Such a mechanism provides an attractive explanation for preferred reversal paths because the geographic location and structure of the induced field are fixed by the distribution of electrical conductivity in the lower mantle. Costin and Buffett (2004) explored this mechanism using a distribution of electrical conductivity that was based on estimates of topography on the CMB (dominantly a degree-2 pattern in spherical harmonics). The main part of the induced field had a nonzonal degree-3 pattern, which was superimposed on a decreasing axial dipole field to predict VGP paths. Preferred paths were caused by the nonzonal part of the field, although the actual location of the preferred paths depended on the location of the observing sites. Costin and Buffett (2004) used the location of sites in the sediment database of Clement (1991) to predict a clustering of reversal paths through the Americas and Asia (see **Figure 6**). This prediction was broadly consistent with inferences drawn from the observations (Clement, 1991).

An interesting test of this prediction is afforded by the current rate of decrease in the dipole field, which is not too different from the average rate of decrease during a reversal (perhaps within a factor of 2 or 3). The induced field is both observable and consistent with historical observations of the field, although it is not currently possible to separate contributions from electromagnetic core–mantle interactions and the underlying variations that originate within the core. This ambiguity is a source of concern because the contribution of electromagnetic core–mantle interactions to the field at the Earth's surface can potentially complicate the way we interpret observations of secular variation.

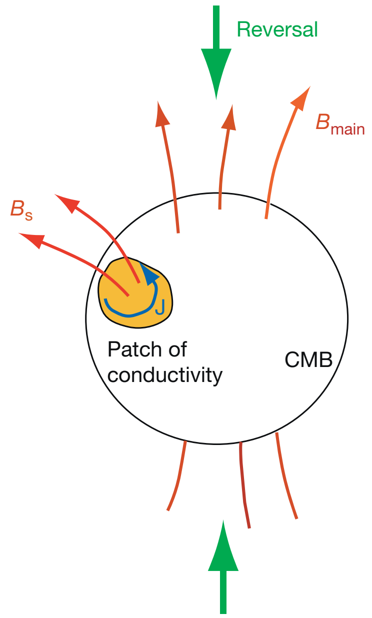

Figure 5 Time variations in the main magnetic field, B_{main}, during reversals induce electric currents J in the conductive regions at the CMB. The electric currents generate a secondary field, B_s, which is superimposed on B_{main}. The resulting distortion of B_{main} can give rise to preferred reversal paths because the location of the secondary field is fixed by the spatial distribution of electrical conductivity near the base of the mantle.

8.08.4 Mechanical Interactions

Mechanical interactions are commonly invoked to transfer momentum between the core and the mantle. Most attention has focused on mechanisms that account for the observed variations in the length of day over timescales of several decades. Lorentz forces due to electromagnetic interactions offer one possible mechanism, although several other types of mechanical interaction have also been proposed. One such mechanism is due to the flow of the core over topography on the CMB (Hide, 1969). Pressure differences on the leading and trailing sides of bumps on the boundary result in a torque that transfers angular momentum. When seismic estimates of the CMB topography first appeared in the literature (Forte and Peltier, 1991; Morelli and Dziewonski, 1987), it became possible to estimate the pressure (or topographic) torque using models of flow at the top of the core (Hide, 1989; Jault and LeMouel, 1989). Most models of core flow are constrained by assuming a geostrophic force balance in the tangential direction (see **Chapter 8.04**). Under this assumption, the flow field recovered from observations of secular variation can be converted to a pressure field. When that pressure field was

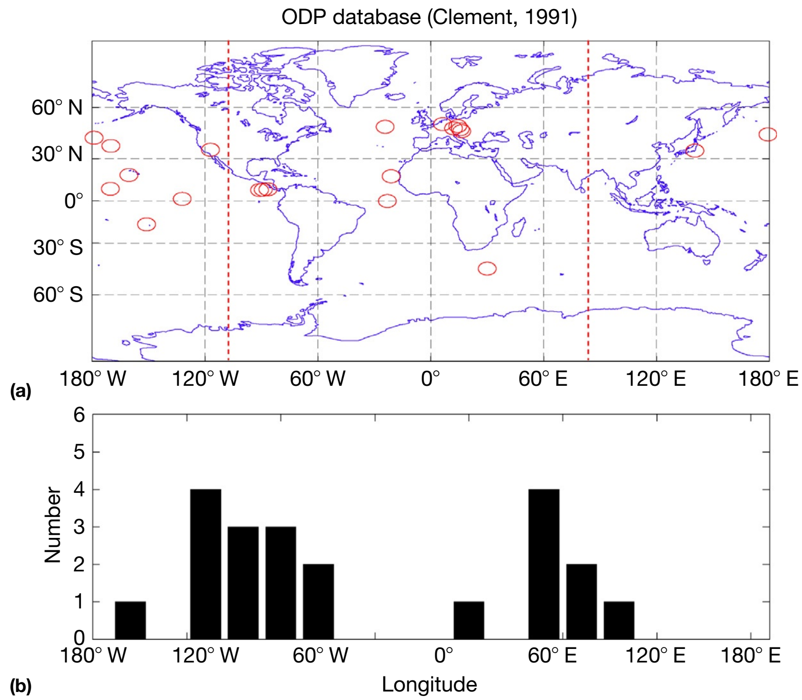

Figure 6 A) Location of samples from the sediment database of Clement (1991) and B) histogram of reversal path longitudes predicted by Costin and Buffett (2004). The spatial distribution of electrical conductivity is based on estimates of the large-scale topography on the CMB. The secondary field induced by this heterogeneous distribution of conductivity causes reversal paths to preferentially pass though the Americas and Asia.

integrated over the boundary with known topography, the resulting torque was too large by several orders of magnitude to explain the observed variation in the length of day (Jault and LeMouel, 1990). A small shift in the position of the topography could greatly reduce the torque, leading to speculations that the pattern of flow was locked by the topography to keep the torque small. Alternatively, it was possible to make small changes to the flow, which eliminated the pressure torque entirely without substantially altering the fit to the secular variation observations (Kuang and Bloxham, 1993). These results demonstrate the sensitivity of the calculation to small errors in either the topography or the flow models.

More problematic is the consistency of calculating a pressure torque using flow models that assume a geostrophic force balance at the top of the core. Geostrophic flow represents a balance between the Coriolis force and pressure gradient. Such a flow can have no time variation because the presence of accelerations implies a departure from geostrophic conditions. There can also be no net torque on the core (or the mantle) because a net torque also implies a change in momentum. Kuang and Bloxham (1997) used this result to show that the pressure torque due to a geostrophic flow must vanish. They did this by demonstrating that the torque associated with the Coriolis force is identically zero. The sum of the pressure and Coriolis torques must vanish if there is no change in momentum in a geostrophic flow, so it follows that the pressure torque is zero. Of course, it is possible that the flow at the top of the core is not geostrophic, so the pressure torque need not vanish. Jault and LeMouel (1999) argued that the geostrophic approximation would still provide a good approximation for the actual pressure field (and hence the pressure torque). However, it is doubtful that a reliable pressure field for mechanical coupling calculations can be recovered from the flow, given the sensitivity of the calculation to small errors.

Other estimates of the pressure torque have been obtained using models of idealized flow over boundary topography (e.g., Anufriyev and Braginsky, 1975, 1977; Moffatt and Dillon, 1976). Pressure in the fluid is perturbed by the flow around the topography. The influence of this perturbation on the boundary topography produces the pressure torque. The amplitude of the pressure torque in these calculations varies as h^2, where h is the height of the topography. One factor of h arises because the perturbation depends on the height of the topography; the second factor of h arises because the integral over the surface for the pressure torque depends on the presence of topography. For boundary topography of a few kilometers at large spatial scales, the resulting pressure torque is probably too small to explain the observed variations in the length of day (e.g., Mound and Buffett, 2005). Similar conclusions have been obtained using numerical geodynamo models that include the influence of boundary topography (Kuang and Chao, 2001). An important aspect of the study by Kuang and Chao (2001) is that they avoid the use of idealized flow and make no assumptions about the structure of the magnetic field. The pressure at the boundary evolves in response to both the underlying convection and the presence of boundary topography. The fact that the pressure torque in these calculations is small would seem to argue against a prominent role for topographic coupling.

Other consequences of fluid pressure on the CMB can be detected at the surface. For example, fluctuations in pressure produce observable changes in both gravity and surface topography (Dumberry and Bloxham, 2004; Fang et al., 1996;

Greff-Lefftz et al., 2004). A typical pressure of 10^3 Pa changes on timescales of several decades as the flow evolves at the CMB. When the mantle responses elastically to the pressure change, the surface displacement can be a few millimeters. The corresponding change in the gravity field is within current the limits of detection (Dumberry and Bloxham, 2004; Greff-Lefftz et al., 2004). Recent interest in this process is motivated by observations of decadal changes in the elliptical part of the gravity field (Cox and Chao, 2002). While it appears that pressure changes in the core are too small to explain the observations of Cox and Chao (2002), current advances in space geodetic observations hold the promise of making the somewhat smaller core processes observable at the Earth's surface.

Gravitational interactions between the core and the mantle cause a different type of mechanical coupling. Convection in both regions creates density anomalies inside the Earth. Gravitational attraction of these density anomalies can result in a transfer of momentum (Jault and LeMouel, 1989; Rubincam, 2003). The distribution of density anomalies in the mantle can be inferred from seismic tomography models by assuming that variations in wave speed are due mainly to temperature (Dziewonski et al., 1977; Hager et al., 1985; Ricard and Vigny, 1989). Unfortunately, a similar procedure is not feasible in the outer core because the density anomalies are far too small to be detected seismically (Stevenson, 1987). An order of magnitude estimate for the density anomalies in the outer core suggests that gravitational interactions could be important (Jault and LeMouel, 1989). However, it is not presently possible to evaluate the torque without knowing the distribution of density anomalies in the outer core.

An alternative source of gravitational interaction occurs between density anomalies in the mantle and the inner core (Buffett, 1996b). The principle source of density heterogeneity in the inner core is caused by topography on the inner-core boundary, which can be estimated by assuming that the boundary tends to adjust over time toward an equipotential surface (see **Chapter 8.12**). (Density anomalies may also occur inside the inner core, but these are probably small compared with the anomalies associated with topography.) In fact, the largest perturbations in the shape of equipotential surfaces in the core are probably due to density anomalies in the mantle, which are large compared with the typical density anomalies in the outer core (e.g., $\Delta\rho/\rho \sim 10^{-8}$). This means that the distribution of density anomalies in the mantle determines the shape of the inner core (see **Figure 7**). Estimates of the gravity perturbations from dynamic geoid studies (Defraigne et al., 1996; Forte et al., 1994) suggest that the peak-to-peak topography on the inner-core boundary is about 100 m or less. When the inner core rotates through the gravitational field of the mantle, a strong gravitational force acts to restore the inner core to its equilibrium position. An equal and opposite force on the mantle is about two orders of magnitude larger than the gravitational force exerted on the mantle by the outer core (Buffett, 1996b), primarily because the density anomalies associated with inner-core topography are much larger (e.g., $\Delta\rho/\rho \sim 10^{-4}$). These large gravitational forces provide a plausible explanation for the decadal variations in the length of day.

Gravitational interactions cannot be solely responsible for fluctuations in the length of day because the moment of inertia of the inner core is so much smaller than that of the mantle.

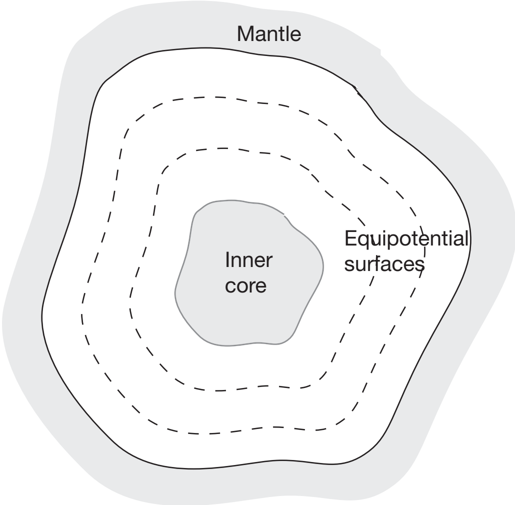

Figure 7 Schematic illustration of the heterogeneous Earth viewed on an equatorial cross section. Density anomalies in the mantle drive flow and perturb the core-mantle boundary. Surfaces of constant potential inside the core are disturbed from axial symmetry by the combined effect of mantle density anomalies and boundary displacements. The inner core adjusts to a hydrostatic state by aligning the boundary with an equipotential surface. This state also minimizes the gravitational potential energy. Rotation of the inner core relative to its equilibrium position produces a mutual gravitational torque on the mantle and inner core.

Instead, the transfer of angular momentum to and from the mantle must rely on changes in the angular momentum of the entire core through a combination of electromagnetic and gravitational torques (Mound and Buffett, 2006). Motions in the fluid outer core are tightly coupled to the inner core by electromagnetic forces on account of the high electrical conductivity on either side of the inner-core boundary. As inner core rotates in response to a strong electromagnetic torque from the fluid core, momentum is transferred to the mantle through the action of the gravitational torque. Tests of this mechanism in numerical geodynamo models yield a torque on the mantle that is sufficient to explain the variations in the length of day (Aubert and Dumberry, 2010; Buffett and Glatzmaier, 2000). It is also possible to explain the length-of-day variations when the fluid motions in the outer core are restricted to the form of torsional oscillations (Dumberry and Mound, 2010; Mound and Buffett, 2005). These oscillations are of interest because the typical period is thought to be compatible with a nominal 60-year variation in the length of day (Braginsky, 1970, 1984). This view has been challenged by a recent detection of torsional oscillations that propagate across the outer core in approximately 4 years (Gillet et al., 2010). Such fast propagation implies a much stronger magnetic field than previously assumed. According to Gillet et al. (2010), these waves recur every 6 years and appear to explain a small-amplitude 6-year variation in the length of day (Abarca del Rio et al., 2000). Alternatively, the 6-year variation might be attributed a gravitational oscillation between the inner core and the mantle (Mound and Buffett, 2006). Corroborating evidence for a gravitationally driven oscillation could be sought in time variations of the gravity field.

8.08.5 Chemical Interactions

It is generally assumed that the core has been chemically isolated from the mantle since the time of core formation. Partial equilibration between liquid iron and silicates establishes the initial composition of the core (e.g., Rubie et al., 2007; Stevenson, 1990). Subsequent transport of mass between liquid iron and silicates is assumed to be insignificant after the core forms. This conventional view is challenged by the studies of Knittle and Jeanloz (1989, 1991), which used diamond-anvil-cell experiments to show that liquid iron reacts with silicates and oxides at high pressure and temperature. The reaction products were thought to include iron alloys, such as FeO and FeSi, and iron-depleted silicate minerals (Goarant et al., 1992; Knittle and Jeanloz, 1989). Mantle minerals in direct contact with the core liquid should quickly establish a local equilibrium because reactions at high temperature are expected to be fast and convective mixing in the core can be relatively efficient (the convective overturn time is probably on the order of 10^3 years). On the other hand, convection in the mantle exposes fresh surfaces of unreacted material more slowly. Jeanloz (1990) suggested that chemical reactions and transport of light elements into the core could have occurred over most of the Earth's history.

Subduction of oxidized ocean crust may also drive reactions by altering chemical conditions at the base of the mantle (Walker, 2005). In either case, chemical reactions could disturb the composition of the core by permitting a flux of mass between the mantle and the core.

Evidence for the core leaking back into the mantle is based on measurements of osmium isotope ratios in lava associated with some hotspots (Brandon et al., 1998; Walker et al., 1995). Enrichment in $^{186}Os/^{188}Os$ and $^{187}Os/^{188}Os$ relative to upper mantle materials has been attributed to small additions of core material to the lower mantle. This core material is subsequently entrained in mantle plumes, where it contributes to lava that is sampled at the surface (see Brandon and Walker, 2005, for a review). Only small amounts of core material are required to perturb the isotopic composition of the mantle because the concentration of Os in the core vastly exceeds that in the mantle, based on partitioning of Os between silicates and liquid metal. However, enrichment in isotopic ratios require a source region with elevated ratios of Pt/Os and Re/Os relative to typical mantle values in order to produce excess ^{186}Os and ^{187}Os through radioactive decay of ^{190}Pt and ^{187}Re. Given the long half-lives involved (e.g., 489 and 42 Ga), the elevated ratios of Pt/Os and Re/Os must be maintained for a very long time to produce the required isotopic enrichment.

Brandon et al. (1998) attributed the elevated ratios of Pt/Os and Re/Os in the liquid core to the growth of the inner core. The initial abundances of Pt, Re, and Os in the core should be close to the chondritic abundances because all of these elements are highly siderophile; most of the initial inventory enters the core with little fractionation. Solidification of the core removes more Os from the liquid core than either Re or Pt (Walker, 2000). This process increases Pt/Os and Re/Os ratios in the outer core above the chondritic ratios. However, experimental estimates for the partitioning of Pt, Re, and Os between liquid and solid iron appear to require an old age for the inner core (Brandon and Walker, 2005), which is incompatible with models for the thermal history of the core (Buffett, 2002; Labrosse et al., 2001). A further complication has arisen with recent measurement of tungsten isotopes in ocean-island basalts that exhibit $^{186}Os/^{188}Os$ and $^{187}Os/^{188}Os$ enrichment (Schersten et al., 2004; Takamasa et al., 2009). So far, there is no evidence for a core signature in tungsten isotopes. On the other hand, Humayun (2011) had proposed a mechanism to elevate ratios of Pt/Os and Re/Os at the base of the mantle after allowing transport of core material across the CMB. This proposal may circumvent the need for an old inner core and avoid difficulties with tungsten isotopes in the mantle. Thus, the role of the core in producing coupled variations in Os isotope ratios remains an open question.

Despite the controversy over isotopic signals from the core, it is difficult to escape the conclusion that some form of chemical interaction is inevitable. Recent experiments on partitioning of major elements between liquid iron and mantle minerals suggest that the core is currently undersaturated in Si and O (Asahara et al., 2007; Ozawa et al., 2008; Sakai et al., 2006; Siebert et al., 2012; Takafuji et al., 2005). For present-day estimates of temperature and bulk mantle composition, the equilibrium concentrations of Si and O in liquid iron should vastly exceed the concentrations required to explain the density deficit of the core relative to pure iron (Tsuno et al., 2013). Transfer of Si and O to the core can produce a buoyant layer at the top of the core (Ozawa et al., 2009), although the vertical extent of such a layer is potentially limited by diffusive transport through the mantle. Most mantle minerals have low diffusivity (Van Orman et al., 2003), but even small amounts of partial melt can substantially enhance diffusivity, eliminating the limitation of mantle-side transport. In this case, a buoyant layer grows by diffusion into the liquid core with modest entrainment by the underlying convection (Buffett and Seagle, 2010).

Cooling over geologic time can substantially alter the solubility of dissolved components. The attendant growth of the inner core can also alter the chemical equilibrium by segregating light elements into the outer core. Eventually, some components in the liquid core may become supersaturated. Stevenson (2007) had argued that Mg is a likely candidate for exsolution because its solubility is relatively low compared with either Si or O. Exsolution could take the form of an immiscible liquid phase (Ito et al., 1995). Alternatively, the excess concentration could drive back reactions at the CMB, removing excess light element and precipitating a solid 'sediment' to the base of the mantle (Buffett et al., 2000). Walker (2005) had also discussed the possibility of electrochemical reactions at the CMB (Kavner and Walker, 2006) and reactions with oxidized oceanic crust. There is no shortage of mechanisms that can cause chemical interactions between the core and the mantle, and there are good reasons for suspecting that many of these operate within the Earth. The challenge lies in quantifying their importance for the evolution and dynamics of the planet.

8.08.6 Conclusions

Interactions between the core and the mantle take many forms. Thermal interaction involves changes in the rate and spatial distribution of heat flow across the CMB. The resulting changes in the vigor and pattern of convection in the core can dramatically affect the geodynamo and produce observable signals in the magnetic field at the Earth's surface. Electromagnetic interactions are the result of electric currents near the boundary. The consequences are entirely dependent on the electrical conductivity of the lower mantle. A conductance of 10^8 S for the lower mantle is sufficient to explain variations in the length of day and to contribute significantly to the induction of magnetic field inside the Earth. Mechanical interactions are most commonly attributed to the effects of fluid pressure acting on the CMB. While pressure torques are not thought to be the primary mechanism for transferring angular momentum between the core and the mantle, deformations due to fluid pressure on the CMB can cause observable changes in gravity and surface displacement. A more viable explanation for the variations in the length of day at decadal periods involves gravitational interactions, primarily between the inner core and the mantle. Better observations of these gravitational interactions may provide new insights into the nonhydrostatic distribution of mass in the mantle. Chemical interactions of some form appear to be likely, although the details are presently unknown. Advances in high-pressure and high-temperature experiments may soon begin to fill in these details and provide unexpected surprises in the chemical evolution of the core.

References

Abarca del Rio R, Gambis D, and Salstein DA (2000) Interannual signals in length of day and atmospheric angular momentum. *Annales Geophysicae* 18: 347–364.

Anufriyev AP and Braginsky SI (1975) Influence of irregularities of the boundary of the Earth's core on the velocity of the liquid and on the magnetic field. *Geomagnetism and Aeronomy* 15: 754–757.

Anufriyev AP and Braginsky SI (1977) Influence of irregularities of the boundary of the Earth's core on fluid velocity and the magnetic field, II. *Geomagnetism and Aeronomy* 17: 78–82.

Asahara Y, Frost DJ, and Rubie DC (2007) Partitioning of FeO between magnesiowustite and liquid iron at high pressures and temperatures: Implications for the composition of the Earth's outer core. *Earth and Planetary Science Letters* 257: 435–449.

Aubert J and Dumberry M (2010) Steady and fluctuating inner core rotation in numerical geodynamo models. *Geophysical Journal International* 184: 162–170.

Badro J, Fiquet G, Guyot F, et al. (2003) Iron partitioning in Earth's mantle: Toward a deep lower mantle discontinuity. *Science* 300: 789–791.

Bloxham J (2002) Time-independent and time-dependent behaviour of high-latitude flux bundles at the core–mantle boundary. *Geophysical Research Letters* 29: 1854. http://dx.doi.org/10.1029/2001GL014543.

Bloxham J and Gubbins D (1987) Thermal core–mantle interactions. *Nature* 325: 511–513.

Bloxham J and Jackson J (1990) Lateral temperature variations at the core–mantle boundary deduced from the magnetic field. *Geophysical Research Letters* 17: 1997–2000.

Braginsky SI (1963) Structure of F layer and reasons for convection in the Earth's core. *Doklady Akademii Nauk SSSR* 149: 1311–1317.

Braginsky SI (1970) Torsional magnetohydrodynamic vibrations in the Earth's core and variations in length of day. *Geomagnetism and Aeronomy* 10: 1–8.

Braginsky SI (1984) Short-period geomagnetic secular variation. *Geophysical and Astrophysical Fluid Dynamics* 30: 1–78.

Brandon AD and Walker RJ (2005) The debate over core–mantle interaction. *Earth and Planetary Science Letters* 232: 211–225.

Brandon AD, Walker RJ, Morgan JW, Norman MD, and Prichard HM (1998) Coupled Os-186 and Os-187 evidence for core–mantle interaction. *Science* 280: 1570–1573.

Buffett BA (1992) Constraints on magnetic energy and mantle conductivity from the forced nutations of the Earth. *Journal of Geophysical Research* 97: 19581–19597.

Buffett BA (1996a) Effects of a heterogeneous mantle on the velocity and magnetic fields at the top of the core. *Geophysical Journal International* 125: 303–317.

Buffett BA (1996b) Gravitational oscillations in the length of day. *Geophysical Research Letters* 23: 2279–2282.

Buffett BA (2002) Estimates of heat flow in the deep mantle based on the power requirements for the geodynamo. *Geophysical Research Letters* 29: 1566. http://dx.doi.org/10.1029/2001GL014649.

Buffett BA, Garnero EJ, and Jeanloz R (2000) Sediments at the top of the core. *Science* 290: 1338–1342.

Buffett BA and Glatzmaier GA (2000) Gravitational breaking of inner-core rotation in geodynamo simulations. *Geophysical Research Letters* 27: 3125–3128.

Buffett BA and Seagle CT (2010) Stratification of the top of the core due to chemical interactions with the mantle. *Journal of Geophysical Research* 115: B04407.

Bullard EC, Freeman C, Gellman H, and Nixon J (1950) The westward drift of the Earth's magnetic field. *Philosophical Transactions of the Royal Society of London, Series A* 132: 61–92.

Bunge HP, Hagelberg CR, and Travis BJ (2003) Mantle circulation models with variational data assimilation: Inferring past mantle flow and structure from plate motion histories and seismic tomography. *Geophysical Journal International* 152: 280–301.

Busse FH and Wicht J (1992) A simple dynamo caused by conductivity variations. *Geophysical and Astrophysical Fluid Dynamics* 62: 135–144.

Calkins MA, Noir J, Eldredge JD, and Aurnou J (2012) The effects of boundary topography on convection in Earth's core. *Geophysical Journal International* 189: 799–814.

Chan KH, Zhang KK, Li LG, and Liao XH (2008) On the effect of an electrically heterogeneous lower mantle on planetary dynamos. *Physics of the Earth and Planetary Interiors* 169: 204–210.

Christensen UR and Olson P (2003) Secular variation in numerical geodynamo models with lateral variations of boundary heat flow. *Physics of the Earth and Planetary Interiors* 138: 39–54.

Clement BM (1991) Geographical distribution of transitional VGPs: Evidence for non-zonal equatorial symmetry during the Matuyama–Brunhes reversal. *Earth and Planetary Science Letters* 104: 48–58.

Clement BM (2004) Dependence of the duration of geomagnetic polarity reversals on site latitude. *Nature* 428: 637–640.

Costin SO and Buffett BA (2004) Preferred reversal paths caused by a heterogeneous conducting layer at the base of the mantle. *Journal of Geophysical Research* 109: B06101. http://dx.doi.org/10.1029/2003JB002853.

Cox CM and Chao BF (2002) Detection of a large-scale mass redistribution in the terrestrial system since 1998. *Science* 297: 831–833.

Davies CJ, Gubbins D, Ashley AP, and Jimack PK (2008) Time-averaged paleomagnetic field and secular variation: Predictions from dynamo solutions based on lower mantle seismic tomography. *Physics of the Earth and Planetary Interiors* 169: 194–203.

de Koker N, Steinle-Neumann G, and Vicek V (2012) Electrical resistance and thermal conductivity of liquid Fe alloys at high P and T, and the heat flux in Earth's core. *Proceedings of the National Academy of Sciences of the United States of America* 109: 4070–4073.

de Wijs GA, Kresse G, Vocadlo L, et al. (1998) The viscosity of liquid iron at the physical conditions of the Earth's core. *Nature* 392: 805–807.

Defraigne P, Dehant V, and Wahr JM (1996) Internal loading of an inhomogeneous compressible earth with phase boundaries. *Geophysical Journal International* 125: 173–192.

Deleplace B and Cardin P (2006) Viscomagnetic torque at the core mantle boundary. *Geophysical Journal International* 167: 557–566.

Driscoll P and Olson P (2011) Superchron cycles driven by variable core heat flow. *Geophysical Research Letters* 38: L09304.

Dumberry M and Bloxham J (2004) Variations in the Earth's gravity field caused by torsional oscillations in the core. *Geophysical Journal International* 159: 417–434.

Dumberry M and Mound J (2010) Inner core–mantle gravitational locking and the super-rotation of the inner core. *Geophysical Journal International* 181: 806–817.

Dziewonski AM, Hager BH, and O'Connell RJ (1977) Large-scale heterogeneities in the lower mantle. *Journal of Geophysical Research* 82: 239–255.

Fang M, Hager BH, and Herring TA (1996) Surface deformation caused by pressure changes in the fluid core. *Geophysical Research Letters* 23: 1493–1496.

Forte AM and Peltier WR (1991) Mantle convection and core–mantle boundary topography – Explanations and implications. *Tectonophysics* 187: 91–116.

Forte AM, Woodward RL, and Dziewonski AM (1994) Joint inversion of seismic and geodynamic data for models of three-dimensional mantle heterogeneity. *Journal of Geophysical Research* 99: 21857–21877.

Gillet N, Jault D, Canet E, and Fournier A (2010) Fast torsional waves and strong magnetic field within the Earth's core. *Nature* 465: 74–77.

Glatzmaier GA, Coe RS, Hongre L, and Roberts PH (1999) The role of the Earth's mantle in controlling the frequency of geomagnetic reversals. *Nature* 401: 885–890.

Goarant F, Guyot F, Peronneau J, and Poirier JP (1992) High-pressure and high-temperature reactions between silicates and liquid iron alloys in the diamond cell studied by analytical electron microprobe. *Journal of Geophysical Research* 97: 4477–4487.

Greff-Lefftz M, Pais MA, and LeMouel JL (2004) Surface gravitational field and topography changes induced by the Earth's fluid core motions. *Journal of Geodesy* 78: 386–392.

Gubbins D and Kelly P (1993) Persistent patterns in the geomagnetic field over the past 2.5 Myr. *Nature* 365: 829–832.

Gubbins D, Thompson CJ, and Whaler KA (1982) Stable regions in the Earth's liquid core. *Geophysical Journal of the Royal Astronomical Society* 68: 241–251.

Hager BH, Clayton RW, Richards MA, Comer RP, and Dziewonski AM (1985) Lower mantle heterogeneity, dynamic topography and the geoid. *Nature* 313: 541–546.

Heller PL, Anderson DL, and Angevine CL (2006) The middle Cretaceous pulse of rapid sea-floor spreading real or necessary? *Geology* 24: 491–494.

Herring TA, Buffett BA, Mathews PM, and Shapiro II (1991) Forced nutations of the Earth: Influence of inner core dynamics, 3. Very long baseline interferometry data analysis. *Journal of Geophysical Research* 96: 8259–8273.

Herring TA, Mathews PM, and Buffett BA (2002) Modeling of nutation and precession: Very long baseline results. *Journal of Geophysical Research* 107: 2069. http://dx.doi.org/10.1029/2001JB000165.

Hide R (1969) Interaction between Earth's liquid core and mantle. *Nature* 222: 1055–1056.

Hide R (1989) Fluctuations in the Earth's rotation and the topography of the core–mantle interface. *Philosophical Transactions of the Royal Society of London, Series A* 328: 351–363.

Holme R (1998) Electromagnetic core–mantle coupling I. Explaining decadal changes in the length of day. *Geophysical Journal International* 132: 167–180.

Humayun M (2011) A model for osmium isotopic evolution of metallic solids at the core–mantle boundary. *Geochemistry, Geophysics, Geosystems* 12: Q03007. http://dx.doi.org/10.1029/2010GC003281.

Ito E, Morooka K, Ujike O, and Katsura T (1995) Reactions between molten iron and silicate melts at high pressure – Implications for the chemical evolution of the Earth's core. *Journal of Geophysical Research* 100: 5901–5910.

Jault D and LeMouel JL (1989) The topographic torque associated with tangentially geostrophic motion at the core surface and inferences on the flow inside the core. *Geophysical and Astrophysical Fluid Dynamics* 48: 273–296.

Jault D and LeMouel JL (1990) core–mantle boundary shape – Constraints inferred from the pressure torque acting between the core and the mantle. *Geophysical Journal International* 101: 233–241.

Jault D and LeMouel JL (1999) Comment on 'On the dynamics of topographical core–mantle coupling'. *Physics of the Earth and Planetary Interiors* 114: 211–215.

Jeanloz R (1990) The nature of the Earth's core. *Annual Review of Earth and Planetary Sciences* 18: 357–386.

Johnson CL and Constable CG (1997) The time-averaged geomagnetic field: Global and regional biases for 0–5 Ma. *Geophysical Journal International* 131: 643–666.

Johnson CL and Constable CG (1998) Persistently anomalous Pacific geomagnetic fields. *Geophysical Research Letters* 25: 1011–1014.

Kanda RVS and Stevenson DJ (2006) Suction mechanism for iron entrainment into the lower mantle. *Geophysical Research Letters* 33: L02310. http://dx.doi.org/10.1029/2005GL025009.

Kavner A and Walker D (2006) Core/mantle-like interactions in an electric field. *Earth and Planetary Science Letters* 248: 316–329.

Knittle E and Jeanloz R (1989) Simulating the core–mantle boundary – An experimental study of high-pressure reactions between silicates and liquid iron. *Geophysical Research Letters* 16: 609–612.

Knittle E and Jeanloz R (1991) The Earth's core–mantle boundary: Results of experiments at high pressure and temperature. *Science* 251: 1438–1443.

Kohler MD and Stevenson DJ (1990) Modeling core fluid motions and the drift of magnetic-field patterns at the CMB by using topography obtained by seismic inversion. *Geophysical Research Letters* 17: 1473–1476.

Koot L, Dumberry M, Rivoldini A, de Viron O, and Dehant V (2010) Constraints on the coupling at the core–mantle and inner-core boundaries inferred from nutation observations. *Geophysical Journal International* 182: 1279–1294.

Koot L, Rivoldini A, de Viron O, and Dehant V (2008) Estimation of Earth interior parameters from a Bayesian inversion of very long baseline interferometry. *Journal of Geophysical Research* 113: B08414.

Koyama T, Shimizu H, and Utada H (2001) Possible effects of lateral heterogeneity in the D″ layer on electromagnetic variations of core origin. *Physics of the Earth and Planetary Interiors* 129: 99–116.

Kuang W and Bloxham J (1993) On the dynamics of topographical core–mantle coupling. *Geophysical and Astrophysical Fluid Dynamics* 72: 161–195.

Kuang W and Bloxham J (1997) On the dynamics of topographical core–mantle coupling. *Physics of the Earth and Planetary Interiors* 99: 289–294.

Kuang W and Chao BF (2001) Topographic core–mantle coupling in geodynamo modeling. *Geophysical Research Letters* 28: 1871–1874.

Kutzner C and Christensen UR (2004) Simulated geomagnetic reversals and preferred virtual geomagnetic pole paths. *Geophysical Journal International* 157: 1105–1118.

Labrosse S, Poirier JP, and LeMouel JL (2001) The age of the inner core. *Earth and Planetary Science Letters* 190: 111–123.

Laj C, Mazaud A, Weeks R, Fuller M, and Herrero-Bervera E (1991) Geomagnetic reversal paths. *Nature* 351: 447.

Lay T, Hernlund J, and Buffett BA (2008) Core–mantle boundary heat flow. *Nature Geoscience* 1: 25–32.

Lister JR and Buffett BA (1998) Stratification of the outer core at the core–mantle boundary. *Physics of the Earth and Planetary Interiors* 105: 5–19.

Lithgow-Bertelloni C and Richards MA (1998) The dynamics of Cenozoic and Mesozoic plate motions. *Reviews of Geophysics* 36: 27–78.

Loper DE (1978) Some consequences of a gravitationally powered dynamo. *Journal of Geophysical Research* 83: 5961–5970.

Mathews PM, Buffett BA, Herring TA, and Shapiro II (1991) Forced nutations of the Earth – Influence of inner core dynamics, 1. Theory. *Journal of Geophysical Research* 96: 8219–8242.

Mathews PM and Guo JY (2005) Viscoelectromagnetic coupling in precession-nutation theory. *Journal of Geophysical Research* 110: B02402. http://dx.doi.org/10.1029/JB002915.

Mathews PM, Herring TA, and Buffett BA (2002) Modeling of nutation and precession: New nutation series for nonrigid Earth and insights into the Earth's interior. *Journal of Geophysical Research* 107(B4): 2068. http://dx.doi.org/10.1029/2001JB000390.

Mathews PM and Shapiro II (1992) Nutations of the Earth. *Annual Review of Earth and Planetary Sciences* 20: 469–500.

McNamara AK and Zhong SJ (2005) Thermochemical structures beneath Africa and the Pacific Ocean. *Nature* 437: 1136–1139.

Moffatt HK and Dillon RF (1976) Correlation between gravitational and geomagnetic fields caused by interaction of core fluid motion with a bumpy core–mantle interface. *Physics of the Earth and Planetary Interiors* 13: 67–78.

Morelli A and Dziewonski AM (1987) Topography of the core–mantle boundary and lateral homogeneity of the liquid core. *Nature* 325: 638–678.

Mound JE and Buffett BA (2005) Mechanisms of core–mantle angular momentum exchange and the observed spectral properties of torsional oscillations. *Journal of Geophysical Research* 110: B08103. http://dx.doi.org/10.1029/2004JB0035555.

Mound JE and Buffett BA (2006) Detection of a gravitational oscillation in length of day. *Earth and Planetary Science Letters* 243: 383–389.

Murakami M, Hirose K, Kawamura K, Sata N, and Ohishi Y (2004) Post-perovskite phase transition in $MgSiO_3$. *Science* 304: 855–858.

Nimmo F and Stevenson DJ (2000) Influence of early plate tectonics on the thermal evolution and magnetic field of Mars. *Journal of Geophysical Research* 105: 11969–11979.

Oganov AR and Ono S (2004) Theoretical and experimental evidence for a postperovskite phase of $MgSiO_3$ in Earth's D" layer. *Nature* 430: 445–448.

Ohta K, Hirose K, Ichiki M, Shimizu K, Sata N, and Ohishi Y (2010) Electrical conductivities of pyrolitic mantle and MORB materials up to the lowermost mantle conditions. *Earth and Planetary Science Letters* 289: 497–502.

Olson P and Christensen UR (2002) The time-averaged magnetic field in numerical dynamos with non-uniform boundary heat flow. *Geophysical Journal International* 151: 809–823.

Olson P, Coe RS, Driscoll PE, Glatzmaier GA, and Roberts PH (2010) Geodynamo reversal frequency and heterogeneous core–mantle boundary heat flow. *Physics of the Earth and Planetary Interiors* 180: 66–79.

Olson P, Deguen R, Hinnov LA, and Zhong SJ (2013) Controls on geomagnetic reversals and core evolution by mantle convection in the Phanerozoic. *Physics of the Earth and Planetary Interiors* 214: 87–103.

Ono S, Oganov AR, Koyama T, and Shimizu H (2006) Stability and compressibility of the high-pressure phases of Al_2O_3 up to 200 GPa: Implications for the electrical conductivity of the base of the lower mantle. *Earth and Planetary Science Letters* 246: 326–335.

Otsuka K and Karato SI (2012) Deep penetration of molten iron into the mantle caused by a morphological instability. *Nature* 492: 243–246.

Ozawa H, Hirose K, Mitome Y, Bando Y, Sata H, and Ohishi Y (2008) Chemical equilibrium between ferropericlase and molten iron to 134 GPa and implications for the iron content at the bottom of the mantle. *Geophysical Research Letters* 35: L05308.

Ozawa H, Hirose K, Mitome M, Bando Y, Sata N, and Ohishi Y (2009) Experimental study of reaction between perovskite and molten iron to 146 GPa and implications for chemically distinct buoyant layer at the top of the core. *Physics and Chemistry of Minerals* 36: 355–363.

Petford N, Yuen D, Rushmer T, Brodholt J, and Stackhouse S (2005) Shear-induced material transfer across the core–mantle boundary aided by the post-perovskite phase transition. *Earth Planets Space* 57: 459–464.

Poirier JP and LeMouel JL (1992) Does infiltration of core material into the lower mantle affect the observed geomagnetic field? *Physics of the Earth and Planetary Interiors* 99: 1–17.

Pozzo M, Davies C, Gubbins D, and Alfe D (2012) Thermal and electrical conductivity of iron at Earth's core conditions. *Nature* 485: 355–358.

Ricard Y and Vigny C (1989) Mantle dynamics with induced plate tectonics. *Journal of Geophysical Research* 94: 17543–17559.

Rochester MG (1962) Geomagnetic core–mantle coupling. *Journal of Geophysical Research* 67: 4336–4833.

Roden RB (1963) Electromagnetic core–mantle coupling. *Geophysical Journal of the Royal Astronomical Society* 7: 361–374.

Rowley DB (2002) Rate of plate creation and destruction: 180 Ma to present. *Geological Society of America Bulletin* 114: 927–933.

Rubie DC, Melosh HJ, and Nimmo F (2007) Formation of the Earth's core. In: Stevenson D (ed.) *Treatise on Geophysics*, is Elsevier B.V., vol. 9, pp. 51–90.

Rubincam DP (2003) Gravitational core–mantle coupling and the acceleration of the Earth. *Journal of Geophysical Research* 108: 2338. http://dx.doi.org/10.1029/2002JB002132.

Sakai T, Kondo T, Ohltani E, et al. (2006) Interaction between iron and post-perovskite at core–mantle boundary and core signature in plume source region. *Geophysical Research Letters* 33: L15317.

Sarson GR, Jones CA, and Longbottom AW (1997) The influence of boundary region heterogeneity on the geodynamo. *Physics of the Earth and Planetary Interiors* 101: 13–32.

Schersten A, Elliot T, Hawkesworth C, and Norman M (2004) Tungsten isotope evidence that mantle plumes contain no contribution from the Earth's core. *Nature* 427: 234–237.

Siebert J, Badro J, Antonangeli D, and Ryerson FJ (2012) Metal-silicate partitioning of Ni and Co in a deep magma ocean. *Earth and Planetary Science Letters* 321–322: 189–197.

Sreenivasan B and Gubbins D (2008) Dynamos with weakly convecting outer layers: Implications for core–mantle boundary interaction. *Geophysical and Astrophysical Fluid Dynamics* 102: 395–407.

Stevenson DJ (1987) Limits on lateral density and velocity variations in the Earth's outer core. *Geophysical Journal of the Royal Astronomical Society* 88: 311–319.

Stevenson DJ (1990) Fluid dynamics of core formation. In: Newson H and Jones JH (eds.) *The Origin of the Earth*, pp. 231–249. London: Oxford Press.

Stevenson DJ (2007) Core exsolution: A likely consequence of giant impacts and a likely energy source for the geodynamo. *Eos, Transactions American Geophysical Union* 88(52), Fall Meet. Suppl. Abstract U21D02.

Stix M and Roberts PH (1984) Time-dependent electromagnetic core–mantle coupling. *Physics of the Earth and Planetary Interiors* 36: 49–60.

Sumita I and Olson P (1999) A laboratory model for convection in Earth's core driven by a thermally heterogeneous mantle. *Science* 286: 1547–1549.

Sumita I and Olson P (2002) Rotating thermal convection experiments in a hemispherical shell with heterogeneous boundary heat flux: Implications for the Earth's core. *Journal of Geophysical Research* 107(B8): 2169.

Takafuji N, Hirose K, Mitome M, and Bando Y (2005) Solubilities of O and Si in liquid iron in equilibrium with (Mg, Fe)SiO_3 and the light element in the core. *Geophysical Research Letters* 32: L06313.

Takamasa A, Nakai S, Sahoo Y, Hanyu T, and Tatsumi Y (2009) W isotope composition of oceanic island basalts from French Polynesia and their meaning for core–mantle interaction. *Chem. Geol*. 260: 37–46.

Tsuno K, Frost DJ, and Rubie DC (2013) Simultaneous partitioning of silicon and oxygen into the Earth's core during early Earth differentiation. *Geophysical Research Letters* 40: 66–71.

Valet JP, Fournier A, Courtillot V, and Herrero-Bervera E (2012) Dynamical similarity of geomagnetic reversals. *Nature* 490: 89–93.

Van Orman JA, Fei YW, Hauri EH, and Wang JH (2003) Diffusion in MgO at high pressures: Constraints on deformation mechanisms and chemical transport at the core–mantle boundary. *Geophysical Research Letters* 30: 1056. http://dx.doi.org/10.1029/2002GL016343.

Verhoogen J (1961) Heat balance of the Earth's core. *Geophysical Journal of the Royal Astronomical Society* 4: 276–281.

Wahr JM (1981) The forced nutations of an elliptical, rotating, elastic and oceanless Earth. *Geophysical Journal of the Royal Astronomical Society* 64: 705–727.

Walker D (2000) Core participation in mantle geochemistry. *Geochimica et Cosmochimica Acta* 64: 2897–2911.

Walker D (2005) core–mantle chemical issues. *Canadian Mineralogist* 43: 1553–1564.

Walker RJ, Morgan JW, and Horan MF (1995) ^{187}Os enrichment in some plumes: Evidence for core–mantle interaction. *Science* 289: 819–822.

Wicht J and Jault D (1999) Constraining electromagnetic core–mantle coupling. *Physics of the Earth and Planetary Interiors* 111: 161–177.

Xu X, Lithgow-Bertelloni C, and Conrad CP (2006) Global reconstructions of Cenozoic seafloor ages: Implications for bathymetry and sea level. *Earth and Planetary Science Letters* 243: 552–564.

Xu Y, Shankland TJ, and Poe BT (2000) Laboratory-based electrical conductivity in the Earth's mantle. *Journal of Geophysical Research* 105: 27865–27875.

Zhang K and Gubbins D (1993) Convection in a rotating spherical shell with an inhomogeneous temperature boundary condition: Condition at infinite Prandtl number. *Journal of Fluid Mechanics* 250: 209–232.

Zhang K and Gubbins D (1996) Convection in a rotating spherical fluid shell with an inhomogeneous temperature boundary condition at finite Prandtl number. *Physics of Fluids* 8: 1141–1148.

Zhang YG and Guo GJ (2000) Molecular dynamics calculations of the bulk viscosity of liquid iron-nickel alloy and the mechanisms for the bulk attenuation of seismic waves in the Earth's outer core. *Physics of the Earth and Planetary Interiors* 122: 289–298.

Zhang K and Schubert G (2000) Teleconvection: Remotely driven thermal convection in rotating stratified spherical layers. *Science* 290: 1944–1947.

Zhang N and Zhong S (2011) Heat fluxes at the Earth's surface and core–mantle boundary since Pangea formation and their implications for the geomagnetic superchrons. *Earth and Planetary Science Letters* 306: 205–216.